Kuchar, Joseph; Milne, Glenn; Hill, Alexander; Tarasov, Lev; Nordman, Maaria

An investigation into the sensitivity of postglacial decay times to uncertainty in the adopted ice history

Published in:
Geophysical Journal International

DOI:
10.1093/gji/ggz512

Published: 01/02/2020

Document Version
Publisher's PDF, also known as Version of record

Please cite the original version:
Kuchar, J., Milne, G., Hill, A., Tarasov, L., & Nordman, M. (2020). An investigation into the sensitivity of postglacial decay times to uncertainty in the adopted ice history. *Geophysical Journal International*, *220*(2), 1172-1186. https://doi.org/10.1093/gji/ggz512

Geophysical Journal International

Geophys. J. Int. (2020) **220,** 1172–1186
Advance Access publication 2019 November 15
GJI Geodynamics and tectonics

doi: 10.1093/gji/ggz512

An investigation into the sensitivity of postglacial decay times to uncertainty in the adopted ice history

Joseph Kuchar,[1] Glenn Milne,[2] Alexander Hill,[2] Lev Tarasov[3] and Maaria Nordman[4,5]

[1]*Department of Physics, University of Ottawa, 75 Laurier Ave E, Ottawa, ON K1N 6N5, Canada*
[2]*Department of Earth and Environmental Sciences, University of Ottawa, 75 Laurier Ave E, Ottawa, ON K1N 6N5, Canada. E-mail: gamilne@uottawa.ca*
[3]*Department of Physics and Physical Oceanography, Memorial University of Newfoundland, 230 Elizabeth Ave, St. John's, NL A1C 5S7, Canada*
[4]*Finnish Geospatial Research Institute, National Land Survey of Finland, Kirkkonummi, 02430 Masala, Finland*
[5]*Department of Built Environment, School of Engineering, Aalto University, 02150 Espoo, Finland*

Accepted 2019 November 14. Received 2019 October 18; in original form 2019 April 5

SUMMARY

At the centres of previously glaciated regions such as Hudson Bay in Canada and the Gulf of Bothnia in Fennoscandia, it has been observed that the sea level history follows an exponential form and that the associated decay time is relatively insensitive to uncertainty in the ice loading history. We revisit the issue of decay time sensitivity by computing relative sea level histories for Richmond Gulf and James Bay in Hudson Bay and Ångerman River in Sweden for a suite of reconstructions of the North American and Fennoscandian Ice Sheets and Earth viscosity profiles. We find that while some Earth viscosity models do indeed show insensitivity in computed decay times to the ice history, this is not true in all cases. Moreover, we find that the location of the study site relative to the geometry of the ice sheet is an important factor in determining ice sensitivity, and based on our set of ice sheet reconstructions, conclude that the location of James Bay is not well-suited to a decay time analysis. We describe novel corrections to the RSL data to remove the effects associated with the spatial distribution of sea level indicators as well as for other signals unrelated to regional ice loading (ocean loading, rotation and global mean sea level changes) and demonstrate that they can significantly affect the inference of viscosity structure. We performed a forward modelling analysis based on a commonly adopted 2-layer, sublithosphere viscosity structure to determine how the solution space of viscosity models changes with the input ice history at the three study sites. While the solution spaces depend on ice history, for both Richmond Gulf and Ångerman River there are regions of parameter space where solutions are common across all or most ice histories, indicating low ice load sensitivity for these mantle viscosity parameters. For example, in Richmond Gulf, upper mantle viscosity values of (0.3–0.5)x10^{21} Pa s and lower mantle viscosity values of (5–50)x10^{21} Pa s tend to satisfy the data constraint consistently for most ice histories considered in this study. Similarly, the Ångerman River solution spaces contain a solution with an upper mantle viscosity of 0.3 $\times$ 10^{21} Pa s and lower mantle viscosity values of (5–50)x10^{21} Pa s common to 9 of the 10 ice histories considered there. However, the dependence of the viscosity solution space on ice history suggests that joint estimation of ice and Earth parameters is the optimal approach.

Key words: Loading of the Earth; Sea level change; Rheology: mantle.

1 INTRODUCTION

The Earth's response to the transportation of mass between the oceans and continents during glacial cycles includes deformation of the solid Earth as well as perturbations to the Earth's gravitational field and rotation vector. This mass transfer comprises both the surface ice-ocean mass exchanges and the resulting deformation of the solid Earth. This process is termed glacial isostatic adjustment (GIA), and is the dominant control on sea level changes on 1–10 ka timescales during the transition from glacial to interglacial conditions.

The key inputs to a model of GIA are a history of ice loading to force the model and an Earth viscosity model to determine how the Earth will deform in response to the applied load. These parameters are generally not well known in advance, and so a typical study will proceed by either (i) generating output and comparing to

observables to constrain Earth rheology given an assumed ice history, (ii) determining an Earth viscosity model independently and using the data to constrain the ice history or else (iii) a joint inversion to determine the combination of ice history and Earth rheology that best fit the data. Studies of the first type proceed by using as input one or more previously determined ice histories and varying earth model parameters to compare to observables, most commonly RSL (e.g. Peltier *et al.* 2002; Steffen & Kauffman 2005; Love *et al.* 2016) or GPS data (e.g. Sella *et al.* 2007). Studies of the 2nd type proceed by using observations that are insensitive to variations in the ice history to constrain the Earth viscosity model, before using observations to constrain the ice history. For example the VM1 (Peltier 1996) and VM2 (Peltier 2004) radial viscosity models are designed to satisfy postglacial decay time observations (which are the focus of this study and will be discussed in more detail below) and are subsequently further validated by comparing to a broader range of GIA observables. In the third approach, optimal earth and ice model components are jointly determined by, for example, assuming an initial ice history that can be scaled regionally and searching for combinations of scaling parameters and Earth rheologies that minimize the data misfit (e.g. Lambeck *et al.* 1998, 2017; Caron *et al.* 2017). In most cases, because RSL data are sensitive to both ice and Earth parametrizations, parameter trade-off makes it difficult to independently determine either of these two model inputs, resulting in most inferences of Earth structure based on a GIA analysis being necessarily coupled to the ice history that was used, or vice versa.

As mentioned above, one method of constraining Earth viscosity structure while minimizing dependence on ice history is through the use of postglacial decay times. In previously glaciated regions such as Hudson Bay in Canada or the Gulf of Bothnia in Fennoscandia, it is known that the RSL curves can be approximated by a function of exponential form (McConnell 1968; Andrews 1970; Cathles 1975; Walcott 1980; Mitrovica *et al.* 2000). It has been shown that, while the amplitude of the exponential curve is directly dependent on ice history, the decay constant is relatively insensitive to changes in the ice history (e.g. McConnell 1968; Andrews 1970; Mitrovica & Peltier 1995; Lau *et al.* 2016). This feature has made the RSL observations in Hudson Bay and the Gulf of Bothnia, and their associated decay times, key constraints on Earth rheology in many GIA studies (e.g. Mitrovica & Peltier 1993, 1995; Peltier 2004; Nordman *et al.* 2015; Roy & Peltier 2015; Lau *et al.* 2016; Hill *et al.* 2018). This paper was primarily motivated by the results of a recent study (Hill *et al.* 2018), which demonstrates some sensitivity to decay times in Hudson Bay and Ångerman River (Sweden) to the extent that, in some case, the inferred Earth viscosity models depend on the assumed ice history. While the insensitivity of postglacial decay times to ice history is often cited, there have been relatively few studies probing the extent of the insensitivity, and only one attempt at a systematic investigation involving a large variety of both ice histories and Earth rheologies (Nordman *et al.* 2015, discussed in more detail below). Indeed, it is only relatively recently that the development of glaciological models (e.g. Tarasov *et al.* 2012; Tarasov 2013) has resulted in a significant increase in the number of ice histories available to GIA modellers, making the sort of investigation of Nordman *et al*., or this study, possible.

An excellent overview of the use of the postglacial decay time approximation is found in Mitrovica *et al.* (2000), and here we end this section with a brief discussion centred around the conclusion of the insensitivity of this parameter to variations in the regional ice loading history.

For a Maxwell Earth, the Love numbers describing the viscoelastic response to an impulse loading in time and point-like in space contain an immediate elastic component, as well as a sum over modes of weighted exponentials (Peltier 1974). For example, the Love number that represents radial deformation is defined as,

$$h_l\ (t) = h_l^E \delta\,(t) + \sum_{k\,=\,1}^{N} r_k^l e^{-s_k^l t}, \tag{1}$$

where h_l^E is the immediate elastic component of the response at spherical harmonic degree l, and the sum contains the non-elastic component of the response as a sum of decaying exponentials with amplitudes r_k^l and inverse decay times s_k^l. The vertical land motion response to a general loading is given by convolving this loading function over time and space with $h_l(t)$. Each element in the sum of N weighted exponential functions with a given decay time represents a so-called 'normal mode' in the modelled Earth response (Tromp & Mitrovica 1999). Representing this response by a single relaxation time is an approximation; however, it provides the basis for a method to estimate mantle viscosity structure from near-field data while minimizing sensitivity to the uncertainty in the ice history.

The sensitivity of postglacial decay times to ice history was investigated in Mitrovica & Peltier (1993) and again in Mitrovica & Peltier (1995). The first study compared decay times inferred from ICE-3G (Tushingham & Peltier 1991), and ICE-1 (Peltier & Andrews 1976), and concluded that the resolution of the data was not enough to differentiate between the ice histories. Similarly, Mitrovica & Peltier (1995) investigated the ice history sensitivity of decay times by computing normalized RSL curves for two very different ice histories (one given by ICE-3G and the other a simple ice disk model) at several sites within Hudson Bay and showing that the decay times for the two ice histories were similar for their assumed Earth rheology (see their Figs 6 and 7). A similar test was performed by Mitrovica (1996), in which RSL curves were computed in Ångerman River and Oslo for a simple ice disk and for ICE-1. In this case, while Ångerman River decay times were insensitive to ice history, the same could not be said for Oslo, demonstrating that the ice sensitivity depended on the choice of study site with respect to the geometry of the ice load. Our goal here is to perform similar sensitivity tests, but with a wider variety of Earth viscosity models and more realistic ice histories. More recently, Nordman *et al.* (2015) computed decay times for a suite of glaciological reconstructions of the Fennoscandian Ice Sheet (FIS) from Tarasov (2013). They found some sensitivity to ice history in their computed decay times (see their Fig. 5), but concluded that the decay times were still relatively insensitive to this parameter. Our analysis is very similar to that of Nordman *et al.*, and our results are compatible in that we find some sensitivity in the computed decay times to variations in the ice history. Our main goal here is to explore this sensitivity and its consequences for inferring viscosity structure. It has often been stated that decay times are relatively insensitive to changes in the adopted ice history and previous studies have demonstrated that this is true when compared to the case of using 'raw' RSL data. Here, we aim to explore the extent of this sensitivity in an absolute sense; that is, compared to the baseline of complete insensitivity.

2 METHODOLOGY

2.1 The GIA model

We use a model of GIA to compute sea level changes and Earth deformation. The GIA model inputs are a history of ice loading and an Earth rheology to describe the deformation of the Earth in response to a changing load. In total 20 ice histories are implemented: ICE5G (Peltier 2004), the Australian National University (ANU) ice model (e.g. Lambeck 1993; Lambeck *et al*. 1998, 2014, 2017), 10 reconstructions of the North American Ice Sheet (NAIS) from Tarasov *et al.* (2012) that we patch into a background given by ICE5G, and eight reconstructions of the Fennoscandian Ice Sheet (FIS) from Tarasov (2013), also patched in to ICE5G. All ice histories are shown at their 20 ka BP configuration in Figs S1 and S2. An ice history is developed with an assumed Earth viscosity model; ICE5G was developed with the VM2 radial viscosity model (Peltier 2004) and the Tarasov glaciological models were developed with the VM5a viscosity profile (Peltier & Drummond 2008), both of which are constrained by postglacial decay time observations. The ANU ice history, on the other hand, was developed by iteratively inverting for the ice history and Earth rheology simultaneously, without the use of postglacial decay times. All the ice sheet chronologies were constrained against RSL data. Other data types were also used and a brief overview is provided in the following. For more detail, we refer the reader to the references provided above. The Tarasov NAIS and FIS chronologies are from Bayesian calibrations. The calibrations accounted for age uncertainties and subsequent revisions to the Dyke (2004) deglacial margin chronology for the NAIS (Tarasov *et al.* 2012) and used the DATED deglacial margin chronology for the FIS (Hughes *et al*. 2016, which includes maximum and minimum isochrones for each timeslice). ICE5G was also constrained by the Dyke (2004) chronology and an earlier version of the DATED chronology. The ANU NAIS margin chronology is based on iterative revisions to the ICE-1 model reconstruction of Peltier & Andrews (1976) while their FIS margin chronology was based on their own interpretation of geological data. When developing the ANU and Tarasov models, constraints from strandline proxies for pro-glacial lake levels adjacent to the NAIS were also used (Tarasov *et al.* 2012; Lambeck *et al.* 2017).

We assume a spherically symmetric Maxwell viscoelastic model of the Earth (Peltier 1974) where the elastic and density structures are given by PREM (Dziewonski & Anderson 1981) and the viscosity structure is characterized by a very high viscosity lithosphere, and a sublithosphere mantle composed of upper and lower mantle components with a boundary at 670 km and with viscosities that are free parameters in the modelling. We vary upper mantle viscosity (UMV) from 10^{20} to 10^{21} Pa s and the lower mantle viscosity (LMV) from 10^{21} to 5×10^{22} Pa s. We solve the extended sea level equation (Mitrovica & Milne 2003; Kendall *et al.* 2005) and so we include the effects of time-varying shorelines; the feedback of GIA-induced changes in Earth rotation is also incorporated (Milne & Mitrovica 1998; Mitrovica *et al*. 2005). Because our focus is ultimately on determining the ability of sea level data to constrain sublithosphere viscosity independently of ice history, we leave the thickness of the lithosphere at a constant value of 71 km in this study. As noted in previous studies (e.g. Mitrovica & Forte 1997; Lau *et al.* 2016), variations in this earth model parameter, compared to changing upper and/or lower mantle viscosity, has the least impact on decay time estimates.

An assumption in the accuracy of the exponential form for RSL curves is that the solid Earth is in free decay, that is, there are no locally changing loads. Because the ocean is itself a load that changes over the region and timescale of interest (Han & Gomez 2018), we computed decay times for RSL curves for the ice response only. The contribution from the ocean load was modelled and removed from the observations (see Section 2.3). In the rest of this paper, whenever we refer to modelled RSL we mean the component that comes from the ice load in particular, unless we explicitly state otherwise. Another motivation for considering only the ice load is that our results will isolate the sensitivity associated directly with this load and so will be easier to interpret. One drawback of this approach is that our results do not include indirect sensitivity to the ice load through the ocean loading contribution.

2.2 The data

The RSL data used in this study is a compilation of data presented in Mitrovica *et* al. (2000), Nordman *et al*. (2015) and Pendea *et al.* (2010). The Mitrovica *et al.* study included an assessment of published RSL data for the Hudson Bay region, with data in both the Richmond Gulf and James Bay areas. As the James Bay data discussed in Mitrovica *et al*. is likely flawed (see Mitrovica *et al.* 2000; Pendea *et al.* 2010) we consider only the Richmond Gulf data in the Mitrovica *et al.* (2000) database. Furthermore, for consistency, and as recommended by Mitrovica *et al.* (2000), we consider only those data determined from samples of *Mytilus Edulis*. The data comprises 28 index points spanning the last 6 thousand years. The published data are presented with their C14 age in Mitrovica *et al.* (2000) and therefore we calibrated the C14 ages before comparing model output to the data. For the calibration we use the Calib software (Stuiver & Reimer 1993) and the Marine13 curve of Reimer *et al*. (2013, Table S1). The three youngest points are discarded as they are too recent for the calibration to be valid. For James Bay we use the data of Pendea *et al.*, which consists of 6 data points covering the past 7000 yr. The Ångerman River data was compiled by Nordman *et al*. and comprises 23 data points spanning 8000 yr; the majority of these are based on a varve chronology with others dated via C14 methods. We show the locations of the aggregate sites and data distribution for Richmond Gulf and Ångerman River in Fig. 1. The James Bay data locations of Pendea *et al.* are shown in a map only (their Fig. 1) with no tabulated latitude and longitude information provided. Therefore, all of the James Bay data are treated as if they were located at the estimated aggregate site (Fig. 1). The aggregate sites for Richmond Gulf and James Bay are visually estimated midpoints of their respective regions, while the Ångerman site is determined by a weighted mean. The aggregate east longitude, latitude pairs for Richmond Gulf, James Bay, and Ångerman River are (−76.8, 55.86), (−78, 52.8) and (17.473, 63.051) degrees, respectively.

2.3 Curve fitting and data corrections

Model decay times are determined from computed RSL histories using the Scientific Python (SciPy) curvefit routine, which uses least-squares regression to determine fit parameters. The model output is fitted with the equation

$$RSL\ (t) = A\left(e^{-\frac{t}{\tau}} - 1\right). \tag{2}$$

Decay times are obtained from historical data by fitting a modified form of eq. (2) that includes a possible vertical shift (c) to account for systematic error and uncertainty (Mitrovica *et al.* 2000):

$$RSL\ (t) = A\left(e^{-\frac{t}{\tau}} - 1\right) + c. \tag{3}$$

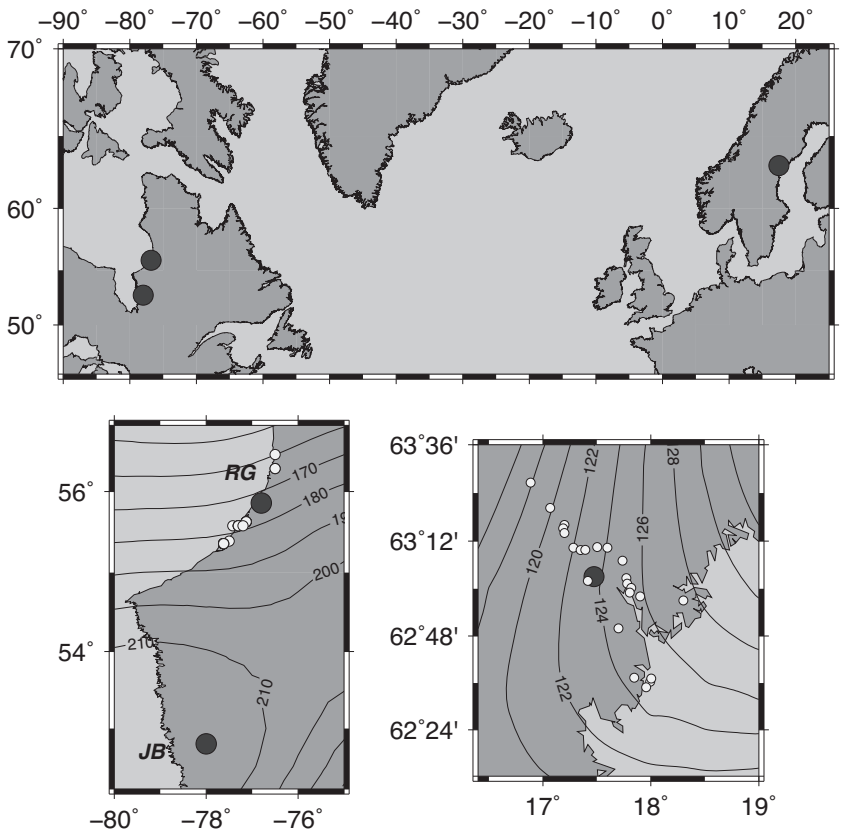

Figure 1. Study areas and locations of sea level index points (white dots) and aggregate sites (large black circles). The aggregate site for James Bay is estimated from Pendea *et al.* (2010). The contours in the lower two figures show a sample calculation of RSL at 7 ka BP for the ICE5G ice history and an earth model with a 71 km lithosphere, 3×10^{20} Pa s UMV and a 10^{22} Pa s LMV. In the lower-left frame, James Bay and Richmond Gulf are abreviated to JB and RG.

These systematic uncertainties may be, for example, displacements related to particularly strong storm surges. The vertical shift was first introduced by Walcott (1980) on the grounds that the sea level data provide a stronger constraint on relative elevation changes between samples than they do on on height relative to present-day mean sea level, and therefore should not be forced to go through the origin at present-day.

Because the historical data contain uncertainties in both altitude and timing, to fit eq. (3) we use SciPy's ODR (Orthogonal Distance Regression) package. Orthogonal distance regression can be considered a generalized least-squares minimization, and the SciPy ODR package is an implementation of the Fortran ODRPACK package (Boggs *et al.* 1989, 1992). This package estimates parameters as well as standard error, which we adopt as the 1σ uncertainty. As a point of comparison, using the Richmond Gulf data and this curve fitting algorithm, we obtain a decay time of 5.5 ± 1.6 ka (see Fig. 2) to 2σ uncertainty, which agrees with the published Richmond Gulf decay times of Mitrovica *et al.* (2000), who report a decay time range of 4–6.6 ka. It should be noted that while we used the ODR package to perform our data-fitting, there are other ways of fitting the data to eq. (4), and the estimates will depend on the method used. For example, we also considered the NLS (non-linear least squares) package in the R statistical programming language (R core team 2018), and on the uncorrected Richmond Gulf data the decay time was estimated to be 4.9 ± 1.8 ka (where the estimate is based on 10 000 model runs). While these estimates agree to within their uncertainties, the differences are larger than we expected. We do not recommend one method over another, but the differences between methods is something to be aware of.

Because the NAIS reconstructions used here are ice free in Hudson Bay by approximately 8 ka BP, to avoid elastic deformation effects we consider the time period from 7 ka BP to present for Hudson Bay. In Fennoscandia, we use an 8 ka window for computing decay times. While Hudson Bay is itself ice free over our study period, some ice persists peripheral to Hudson Bay until approximately 5 ka. We tested the sensitivity of the Hudson Bay sites to ice changes after 7 ka by computing RSL due to those ice changes only and found that the effects were negligible.

A condition for the exponential decay time approximation to be most valid is that the study region is in free decay and is not being influenced by active load changes. One active load is the ice, and this can be dealt with if we consider only a time window after deglaciation. However, sea level indicators are, of course, a measure of sea level, and changes in RSL correspond to changes in the ocean load in the study region. The ocean load is itself a forcing on the Earth that drives sea level change through deformation of the solid Earth and gravitational potential, and this complicates the assumption of free decay. Past studies (Mitrovica *et al.* 2000; Nordman *et al.* 2015) applied corrections to the sea level data to remove the eustatic (meltwater) component of sea level, which produces a global rise in RSL that is independent of the local RSL response and impacts the decay time estimate. The influence of the regional ocean loading—a sea level fall of 100s of metres since the completion of ice melting—has recently been considered by Han & Gomez (2018), who show that the contribution of this load to decay time

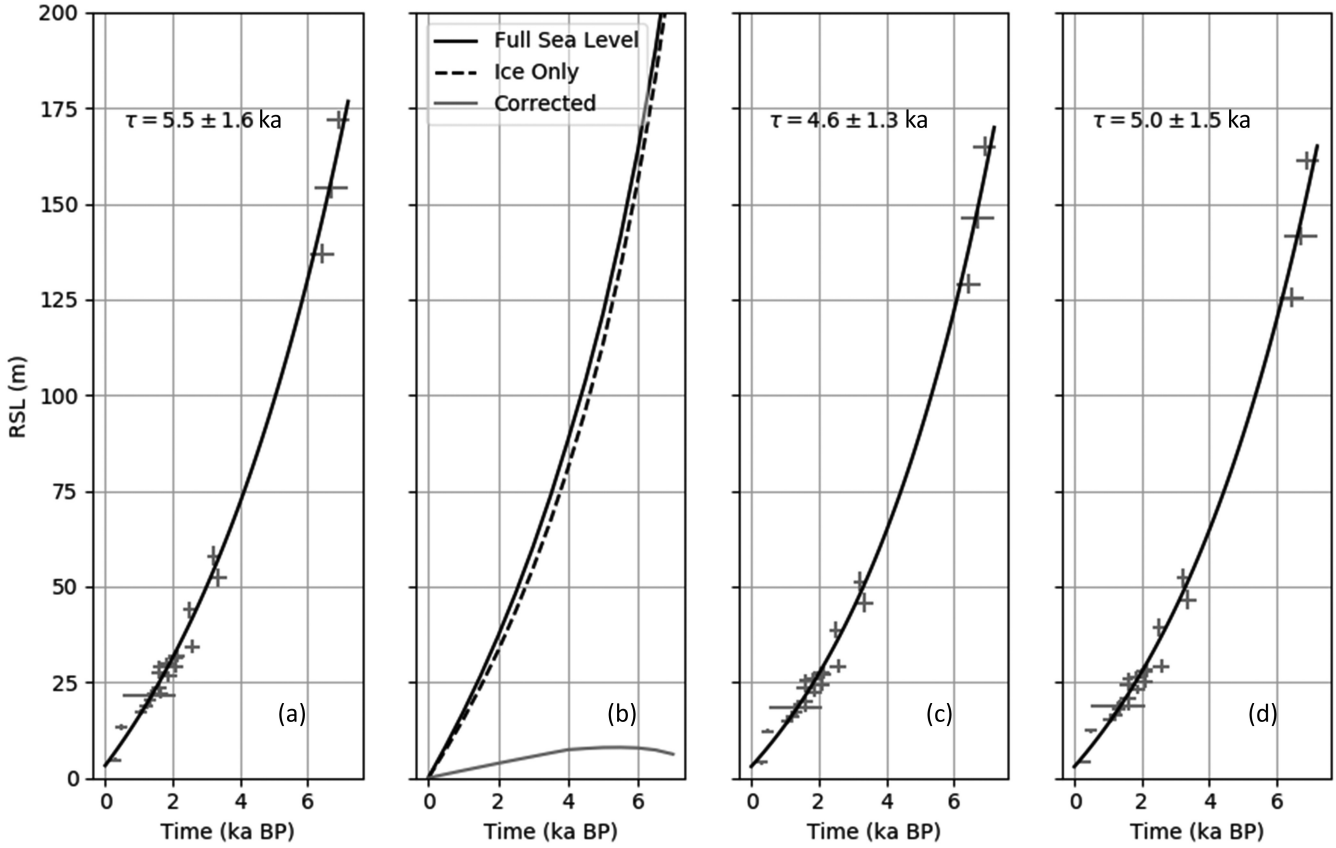

Figure 2. (a) The uncorrected Richmond Gulf data and the best-fitting curve of form defined by eq. (3). (b) The modelled RSL curve including ice, ocean and rotation contributions (solid black), the ice load contribution isolated (dashed black), and the difference between them (grey), for a model run with the 4247 ice history of Tarasov *et al*. (2012), a 71 km lithosphere, a 3×10^{20} Pa s upper mantle and a 10^{22} Pa s lower mantle. When we remove the grey curve in the second frame from the Richmond Gulf data, we obtain the data best-fitting curve in (c). (d) Corrected data of frame (c) with the additional spatial variability correction (see Section 2.3) and the best-fitting curve.

estimates is both non-negligible and spatially variable across the Hudson Bay region. Because the data is a record of all processes that influence sea level, and not only the isostatic response to the ice load in particular, we removed from the observational data all of the contributions except that due to the ice loading for every model parameter set considered. This 'correction' (eq. 4) includes the influence of ocean loading, GIA-induced changes in Earth rotation and changes in global mean sea level associated with ice melting (eustasy) and GIA (syphoning; e.g. Mitrovica & Milne 2003). The model correction applied to the data to account for these effects can be expressed as

$$RSL_{\rm cor} = RSL_{\rm full} - RSL_{\rm ice}, \tag{4}$$

where $RSL_{\rm full}$ represents model output of RSL that incorporates all processes described above and $RSL_{\rm ice}$ is the component due only to the ice load. Because the correction ($RSL_{\rm cor}$) is dependent on the input parameters, the decay time determined from the RSL data is different, in general, for each model run. Essentially, if the model output ($RSL_{\rm full}$) is considered as a sum of an ice loading signal, and an everything-but-the-ice-load signal, then the former is used to determine the model decay time, and the latter (defined by eq. 4) is used as a data correction to determine a data decay time. Fig. 2 (a-c) illustrates the impact of this model correction on the estimated decay time at Richmond Gulf for a given model parameter set. The parameters (3×10^{20} Pa s for UMV and 10^{22} Pa s for LMV) lead to a decrease in the decay time from 5.5 ± 1.6 to 4.6 ± 1.3 ka. For comparison, a model with a more modest viscosity contrast featuring a 10^{21} Pa s UMV and a 10^{22} Pa s LMV leads to a corrected decay time of 5.0 ± 1.4 ka. A second reason to perform this data correction and thus focus on the ice response only is that we are specifically concerned with the sensitivity to this parameter. If the full signal were used to examine decay time variations across ice histories, then the resulting decay times would be influenced not only by the ice variations, but also by the other component signals.

At two of the locations considered (Richmond Gulf and Ångerman River), the data are spread over a large area and so a second model correction was applied to shift the data spatially to their aggregate locations. It is common practice to place data from multiple locations to one for visualization (in the form of a RSL curve) or for curve fitting, but if there is a large gradient in sea level between the actual locations where the data were collected then this can introduce significant error (Nordman *et al.* 2015; Han & Gomez 2018). It was shown by Mitrovica *et al.* (2000) that when data from Richmond Gulf and James Bay are combined into a single curve to determine decay times (as was done in Peltier 1998) it leads to a considerably different decay time than would be found by considering the locations separately. In fact, the RSL difference between the northernmost and southernmost data points in the Richmond Gulf dataset is sufficiently large (up to several tens of metres at 7 ka BP, see lower left frame of Fig. 1) that it significantly affects the estimated decay time. Therefore all data points were shifted by the difference in modelled sea level between the aggregate location and

the actual data location. For example, if modelled RSL at a given time and sea level index point location is computed to be 200 m of RSL and RSL at the aggregate location is computed to be 150 m at the same time step, then that corresponding data point will be shifted by −50 m before the decay time is estimated.

In Fig. 2 (c and d) we illustrate the impact of this spatial correction on estimating the decay time. In this case the decay time is increased by 0.36 ka when this correction is applied for the chosen viscosity model parameters (see caption). For Ångerman River, using the same earth model parameters and the FIS model 78 311 yields an increase in the computed decay time (after application of the correction defined in eq. 4) of 0.43 ka. A similar spatial correction was performed in Nordman *et al*. (2015), except that their correction was determined by sampling the model parameter space and using the maximum differences to determine a single correction, rather than computing parameter-specific data corrections as we do here. The amplitude and sign of the spatial correction will depend on the spatial distribution of the index points relative to the local RSL gradient as well as the adopted model parameter set. Regarding the latter, we note that thinner lithospheres generally result in larger RSL gradients when all other parameter values are fixed, and it is therefore likely that our choice of a relatively thin (71 km) lithosphere will increase the importance of the spatial correction.

The area over which the James Bay data has been collected is significantly smaller (Pendea *et al.* 2010), and comprises only 6 data points, and so the spatial correction is applied only to the Richmond Gulf and Ångerman River data. The correction defined in eq. (4) is applied at all three locations. As a concluding point, it is generally true that the correction defined by eq. (4) lowers the estimated decay time and the spatial correction raises it. This is particularly the case for models with low viscosity in the upper mantle.

3 RESULTS AND DISCUSSION

3.1 Parameter sensitivity investigation

We computed RSL for a suite of Earth rheologies and ice histories. In Fig. 3, we show computed model decay times for all ice histories and a subset of earth models at the three aggregate data locations defined in Fig. 1. For Richmond Gulf, most decay times are fairly closely clustered, typically with a difference of around 500 a for the 2×10^{21} Pa s LMV (left frame), and around 1 ka when the LMV is increased by an order of magnitude (right-hand frame). Uncertainties are not shown in Fig. 3 to avoid cluttering the image, but it should be pointed out that uncertainties typically increase as viscosities and decay times increase. For example, using the 1246 ice history as an example, the 0.5×10^{21} Pa s UMV and 2×10^{21} Pa s LMV best-fitting decay time is 3.36 ± 0.06 ka, and when the LMV is increased to 2×10^{22} Pa s the best-fitting decay time increases to 5.29 ± 0.25 ka. As viscosities increase the modelled curves become more linear, leading to larger parameter uncertainties. For the models shown in Fig. 3 the decay time uncertainties are small compared to the spread from the ice models.

In comparison with Richmond Gulf, the spread of decay times at James Bay is large, particularly for the models featuring a higher viscosity lower mantle. There are differences of decay times among ice models of nearly 3 ka. For Richmond Gulf and James Bay, ICE5G is an outlier for the higher viscosity UMV values, with a decay time significantly below the majority of the rest for both LMV values shown. The Ångerman River decay times exhibit more spread than those of Richmond Gulf, especially for the larger LMV value (right-hand frames). As for the Richmond Gulf and James Bay results, the spread in modelled decay times significantly increases when the LMV is increased by an order of magnitude. There is a general trend of the spread of decay times being larger for the higher LMV models.

While an increase in the spread of decay times is to be expected as the curve-fitting uncertainties increase, the magnitude of spread relative to the size of the uncertainties (not shown) indicates that the decay time sensitivity to the ice model increases at higher viscosities. This reflects the properly that more viscous models have greater relaxation times and so have a longer 'memory' to past ice loading changes.

We extend the results in Fig. 3 to a broader viscosity space in Fig. 4 and show both the mean decay times (where the mean is computed across ice histories) and the spread in decay times across ice histories, which is the difference between the largest and smallest computed decay times. The general structure of the mean (frame (a)) is similar in each of the three locations considered, with the modelled decay time generally increasing with increasing UMV and LMV, but there are also significant differences. As evident in Fig. 3, there is a clear difference in decay times for low UMV and high LMV values between Richmond Gulf and James Bay. The decay time structure of Ångerman is similar to that of Richmond Gulf, except for the region with high UMV values, where the decay times are higher for Ångerman, reflecting a greater sensitivity at the Ångerman location to changes in the UMV (e.g. Lau *et al*. 2016). Also, we do not include the weakest UMV for the Ångerman River results because the computed RSL curves are non-exponential for most ice histories considered [see Hill *et al.* (2018) for more detail on this point]. This is because most of the relaxation occurs before 8 ka as a consequence of the low viscosity values and the relatively early retreat of ice from the region. As it is not reasonable to consider decay times of non-exponential curves, we omit these models from our discussion of the Fennoscandian decay times.

The spread in decay times is shown in frame (b) of Fig. 4. It is generally true for all three sites that the lower/middle left section of parameter space (corresponding to low UMV and LMV values) shows the smallest spread in decay times, with the spread increasing as both UMV and LMV increase. The spread is typically largest for models with high UMV and LMV (top right section of parameter space), except for James Bay, which also features a large spread for the lowest UMV value. The large spread at high UMV values is in part because the RSL curve becomes more linear for higher viscosities, with increasingly large decay times required to fit the modelled behaviour, and so while the differences in decay times are large, the decay times themselves are also large. As the spread shows maximum differences, which may be misleading if there are outlier models, the standard deviation has also been computed, which shows a similar structure to the spread and is provided as Fig. S3.

Richmond Gulf shows a consistently small spread in decay times across the parameter space, except for those models with both high UMV and LMV values. Both James Bay and Ångerman River, however, show considerable spread in decay times, particularly for models with high LMV values. This indicates that Richmond Gulf decay times are relatively insensitive to variations in the input ice history across most of the considered parameter space, with those for Ångerman River and James Bay being more sensitive. This is

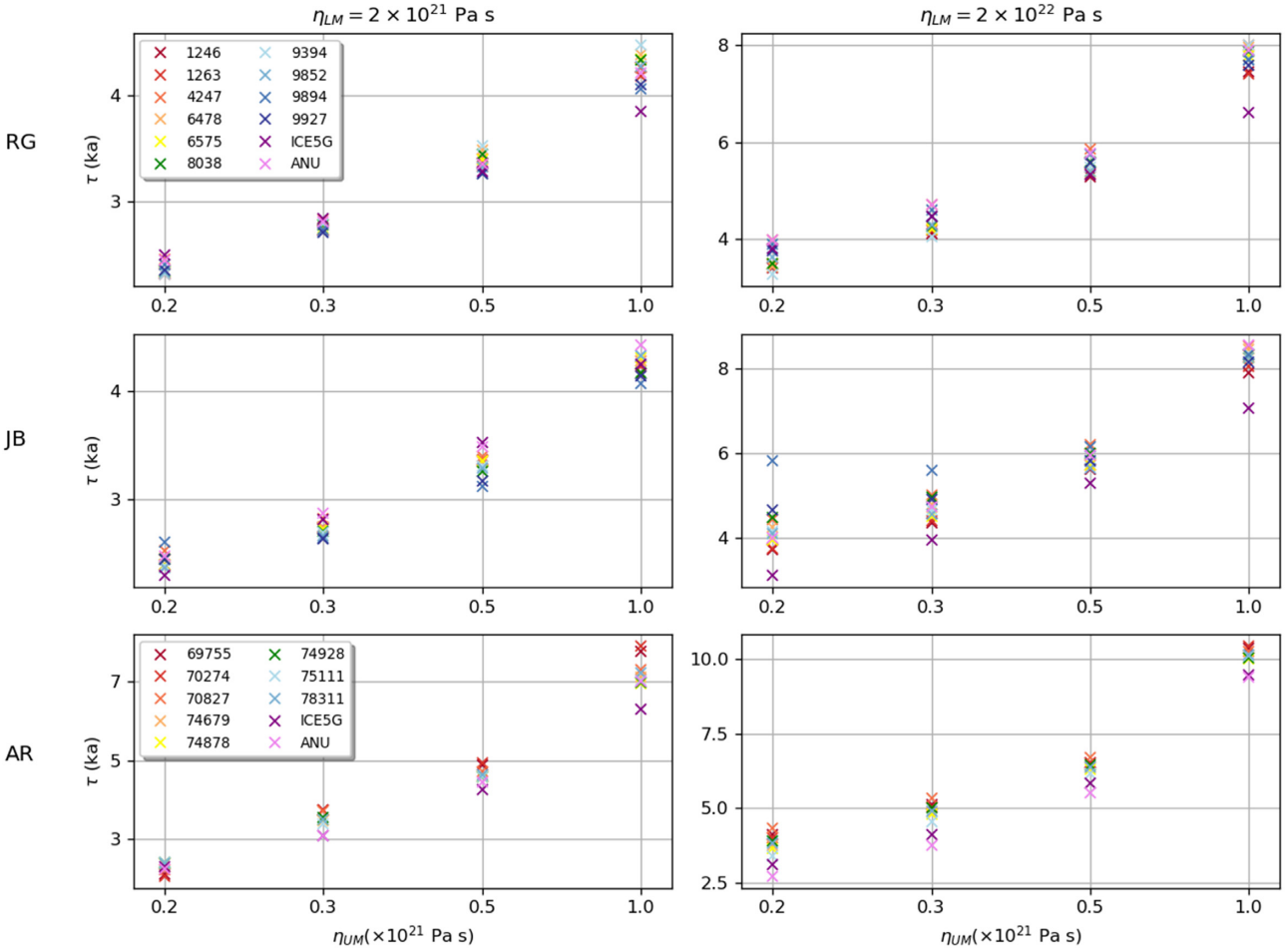

Figure 3. Computed model decay times for all ice histories at Richmond Gulf (RG, top row), James Bay (JB, middle row) and Ångerman River (AR, bottom row). The left-hand column shows results for a LMV of 2 × 10^{21} Pa s while the right-hand column shows output for a LMV of 2 × 10^{22} Pa s. The Richmond Gulf legend also applies to James Bay.

particularly interesting for James Bay, as it is close to Richmond Gulf and so would be expected to show generally similar behaviour. A partial explanation for the noted difference between these two sites follows.

In Fig. 5, we show a spatial plot of RSL at 6 ka BP for all 12 NAIS reconstructions. The first thing to note is that in almost none of these scenarios can both James Bay and Richmond Gulf be considered to be at the centre of the main uplifting region, and often neither can. In fact, for most ice models considered, a centre of uplift would be east of Hudson Bay (i.e. Northern Quebec), which Richmond Gulf is nearer to than James Bay. We say *a* centre of uplift rather than *the* centre of uplift as the Laurentide ice sheet had several domes and there would therefore be multiple centres of uplift (and in the frame showing the RSL of model 9894 there is a second uplifting centre visible in central Hudson Bay). Furthermore, the locations of uplift centres may change over the course of the deglaciation (see Fig. S4). However, comparing uplift patterns for the different ice histories at this time step, Richmond Gulf is generally nearer to a major centre of depression than James Bay, which features significant variety in the type of uplift it is experiencing depending on ice history. We postulate that this consistency in the case of Richmond Gulf and variability in the case of James Bay is reflected in the spread of decay times seen in Fig. 4(b).

3.2 Data model comparison

While we have demonstrated that there is a sensitivity of computed decay times to changes in the input ice sheet history, it is important to determine the impact of this sensitivity when inferring Earth viscosity structure. After all, if the viscosity models most sensitive to ice history do not satisfy the data constraints, then we may conclude that the sensitivity is unimportant.

For every ice history we consider whether a particular earth model is consistent with the data by calculating decay times for the model-generated RSL curves and the model-corrected data (as described in Section 2.3). We then simply determine whether the decay times agree to within the estimated uncertainties determined from the curve fitting routines. We show the results of this exercise for Richmond Gulf, James Bay and Ångerman River in Figs 6–8, respectively (for both 1σ and 2σ uncertainty estimates). Our purpose in this section is not to perform a rigorous inversion for an Earth viscosity model, as we are not taking into account any kind of depth sensitivity of the different ice history/Earth viscosity combinations (e.g. Mitrovica 1996; Lau *et al.* 2016). Rather, our goal is simply to determine how the spread in decay times presented in the previous section can manifest in an inversion that assumes a simplistic, but commonly assumed, two-layer sublithosphere mantle viscosity structure. We are primarily interested in how the solution

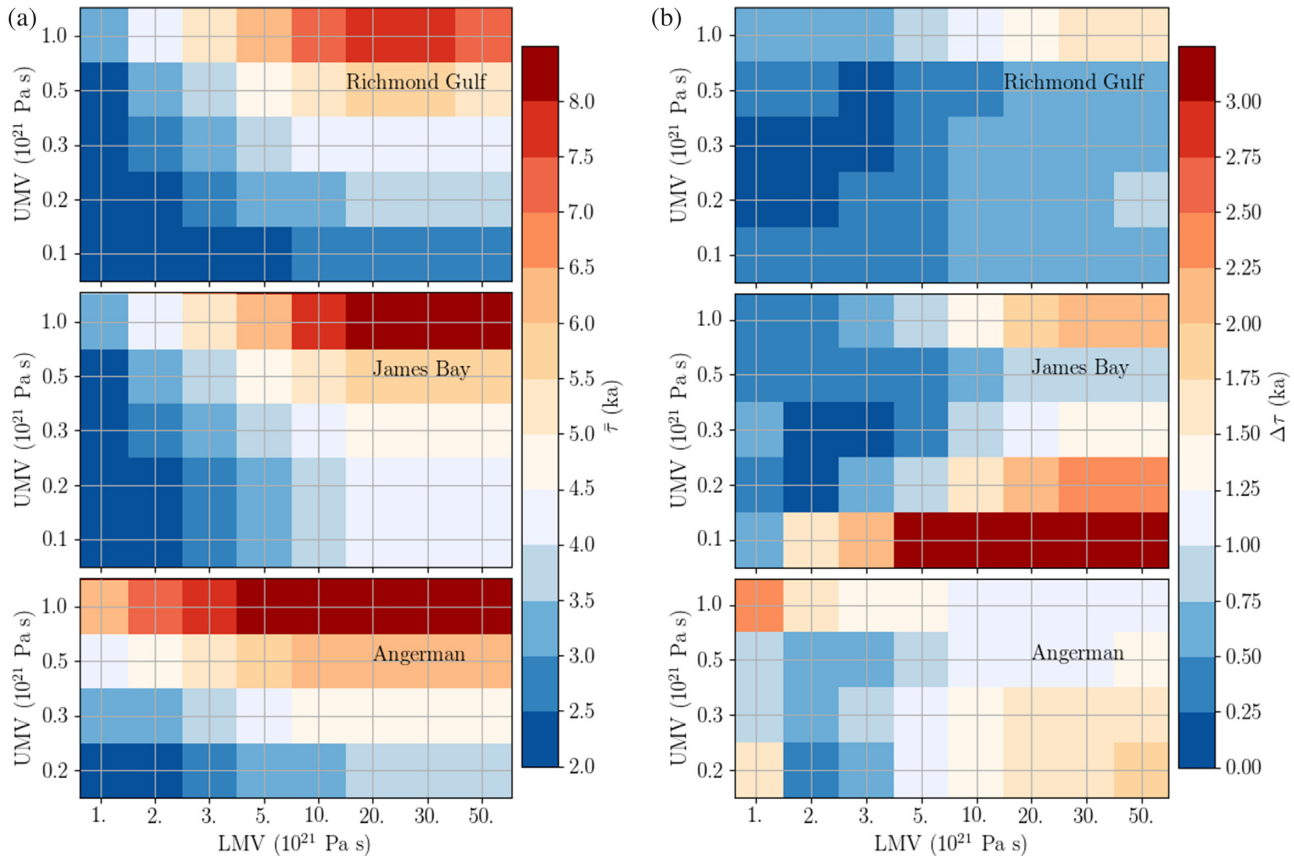

Figure 4. (a) Mean decay times (averaged over the number of ice histories) as a function of upper and lower mantle viscosity. (b) Spread (that is, difference between the largest and smallest) of computed model decay times. The UMV lower limit is not the same for Ångerman as it is for the Hudson Bay sites as the lowest UMV considered resulted in non-exponential RSL behaviour over the 8 ka to present time window for many ice histories (see main text).

space changes, rather than in the solutions themselves. One important limitation of not explicitly considering the data resolving power is that the parameter solution spaces (Figs 6–8) will be broadened due to the greater parameter trade-off in this case, which will lead to an artificial exaggeration of the sensitivity of the results to ice model differences.

What can be seen from these figures is that while each location has an acceptable region of parameter space with a similar shape, there is significant variability among ice histories. For example, for the Richmond Gulf data (Fig. 6), most ice histories show a band of acceptable models with an UMV of 0.2 × 10^{21} Pa s, but this is absent for the 4247 and 8038 histories. Additionally, half of the ice models show a band of acceptable viscosity models with a 10^{21} Pa s UMV, which is absent from the rest. Another interesting feature of the results in Fig. 6 is that the bottom left corner of the parameter space, corresponding to weak UMV and LMV combinations, which was identified in Fig. 4 as being relatively insensitive to variations in ice history, is also a region that does not fit the Richmond Gulf data. That being said, there is generally agreement among ice histories for UMV values of (0.3–0.5)x10^{21} Pa s and higher LMV values satisfying the data, reflecting the low sensitivity seen in the previous section. There is also a region with a UMV value of 0.2 × 10^{21} Pa s and LMV values of (20–50)x10^{21} Pa s, where 10 of the 12 considered ice histories lead to model-data agreement. This indicates that viscosity inferences in this region of parameter space are not significantly influenced by ice history variations. There are also regions of parameter space where only a subset of ice histories lead to model-data agreement, which indicates that there is a sensitivity significant enough to impact a viscosity inversion. For instance, 5 of the 12 ice histories lead to model-data agreement in the region of parameter space with a UMV value of 10^{21} Pa s and LMV values of (30–50)x10^{21} Pa s.

The James Bay decay time constraint results in similarly shaped acceptability regions as seen for Richmond Gulf, but generally shifted to lower UMV values, and significantly narrower (Fig. 7). It may seem counterintuitive that the James Bay model-data agreement space is narrower than for Richmond Gulf, as with only 6 data points we may expect broader parameter estimation uncertainties than is the case for Richmond Gulf, but in fact the opposite is true. While there are relatively few data points in the James Bay dataset, they are typically easily fit with an exponential (such that all points lie on or nearly on the best-fitting curve), while the much larger Richmond Gulf dataset is such that there are always points that are not close to the curve. As a result, the James Bay parameter uncertainties are typically significantly smaller than those determined from the Richmond Gulf dataset (for examples of best-fitting curves for all three sites, see Fig. S5). ICE5G and 9894 are outliers, as neither show the bands of acceptable models of (0.1–0.2)x10^{21} Pa s UMV common among the rest. The results for the 9894 ice history are indicative of how much different the behaviour at James Bay is relative to Richmond Gulf; for Richmond Gulf, the model fits lead to a parameter solution space that looks very similar to those of 9852 and 9927, but for James Bay there is a large change in the acceptability space, with all LMV values higher than 5 × 10^{21} Pa s being rejected. As we have seen in Section 3.1, the James Bay model decay times are relatively sensitive to ice history, and this is also

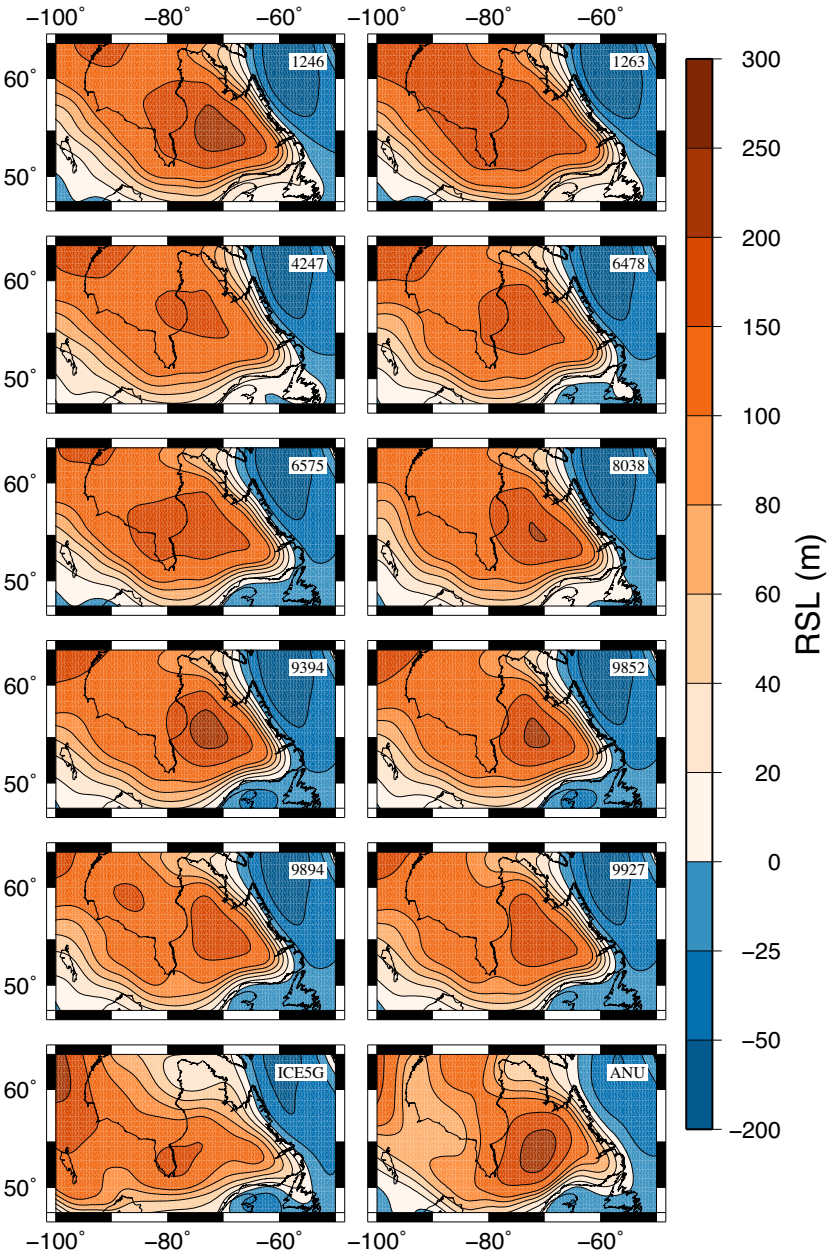

Figure 5. RSL computed at 6 ka BP for 12 different ice models (indicated at top right of each frame) and an earth model with a 71-km-thick lithosphere, 5×10^{20} Pa s UMV and a 10^{22} Pa s LMV.

reflected in the model-data comparison. Unlike Richmond Gulf, where there are many Earth models that satisfy the data constraints common to all ice histories, in the case of James Bay there are no solutions common across all ice histories, though there are solutions with a UMV of 0.2×10^{21} Pa s and LMV values of (10–50)x10^{21} Pa s common to 7 of the 12 ice histories. Given that there is no consistent data-model agreement for most ice histories, and the location is one where the model output shows ice sensitivity independently of the data, we conclude that these data are not well-suited for using decay times to infer Earth viscosity structure.

The Ångerman River data fits (Fig. 8) give a solution region that is consistent with the Richmond Gulf case, which is largely characterized by a low UMV, with structure that varies with ice history. The scale is different from those of James Bay and Richmond Gulf, with a UMV starting at 0.2×10^{21} Pa s. The space of model-data agreement is much smaller than Richmond Gulf, which likely reflects the relatively small age uncertainties of the Ångerman River data (most of which are based on a varve chronology) compared to the larger uncertainties of calibrated C14 ages in the Richmond Gulf data set. Comparing Fig. 8 with Fig. 5 of Nordman *et al.* (2015), who used the same data set but a different suite of ice histories to compute decay times, we see consistent results in that there is general model-data agreement for a 0.3×10^{21} Pa s UMV for high LMV values. There is also some ice history variability in the decay times in the Nordman *et al.* figure, but their choice of scales (for instance, using a single colour for the range 0–4.2 ka) makes variability in those ranges impossible to determine. Such a choice is justifiable on the basis that these decay times are outside of the range inferred from the observational constraints.

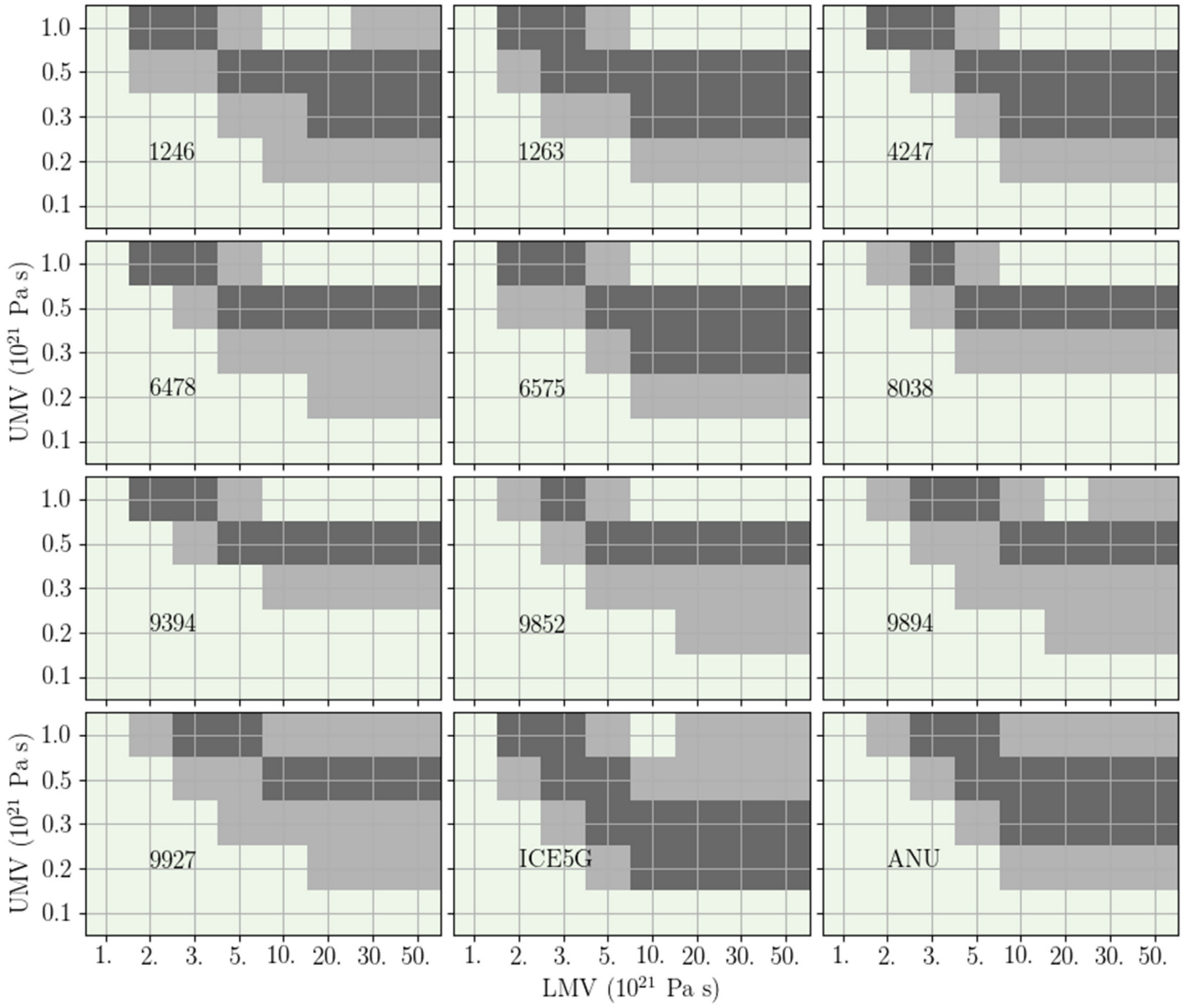

Figure 6. In grey we show the regions of parameter space where the model output decay time agrees with the Richmond Gulf model-corrected data decay time to within uncertainty (1σ in dark grey and 2σ in light grey).

For Ångerman River (Fig. 8) we also see that most ice histories lead to a band of acceptable earth models with a UMV of 0.3×10^{21} Pa s, but ICE-5G also accepts a lower value of 0.2×10^{21} Pa s. All ice histories except for 70827 lead to acceptable earth models with a UMV of 0.3×10^{21} Pa s and a LMV from (5–50)x10^{21} Pa s, similar to one of the classes of solutions of the Richmond Gulf data. However, when the 70827 ice history is included, then the range of acceptable LMV values shrinks to (5–20)x10^{21} Pa s. This demonstrates a low ice sensitivity in this region of parameter space, particularly for LMV values in the range of (5–20)x10^{21} Pa s. There is also a solution of a UMV value of 0.5×10^{21} Pa s and LMV value of 2×10^{21} Pa s common to all 10 ice histories. Given that the numbered ice models were developed with only a single Earth viscosity profile (VM5a), a key future step will be the joint calibration of the ice histories and viscosity models.

Overall, our results are compatible with those of Hill *et al.* (2018), who explored ice model sensitivity as part of an investigation to determine whether postglacial decay times in Richmond Gulf and Ångerman River could constrain earth models featuring a thin low viscosity layer above the mantle transition zone. The Hill *et al.* study considered a much reduced spread of ice histories relative to the present study, but still found evidence of ice history sensitivity. Importantly, the earth models which could be considered to have satisfied the data constraints were dependent on the assumed ice history (for example, see their figs 3, S2 and S3). This is consistent with our own Figs 6–8, and demonstrates that for a practical application, the often-invoked insensitivity of decay times to the input ice model should not be universally assumed. Moreover, here we have considered only a fairly simple class of Earth models featuring a two-layer sublithosphere viscosity structure, and Hill *et al.* observe that the ice sensitivity also exists for more complex three-layer models. That being said, our results also demonstrate that for a significant region of the viscosity parameter space, data from both Richmond Gulf and Ångerman River can be satisfied with a wide variety of ice histories, demonstrating low ice model sensitivity for these viscosity structures.

The primary advantage of the decay time approach is to constrain earth model parameters independently of ice history, but if it becomes necessary to test ice sensitivity as well (as we do here, and as was done in Hill *et al.*), then the primary advantage of using decay

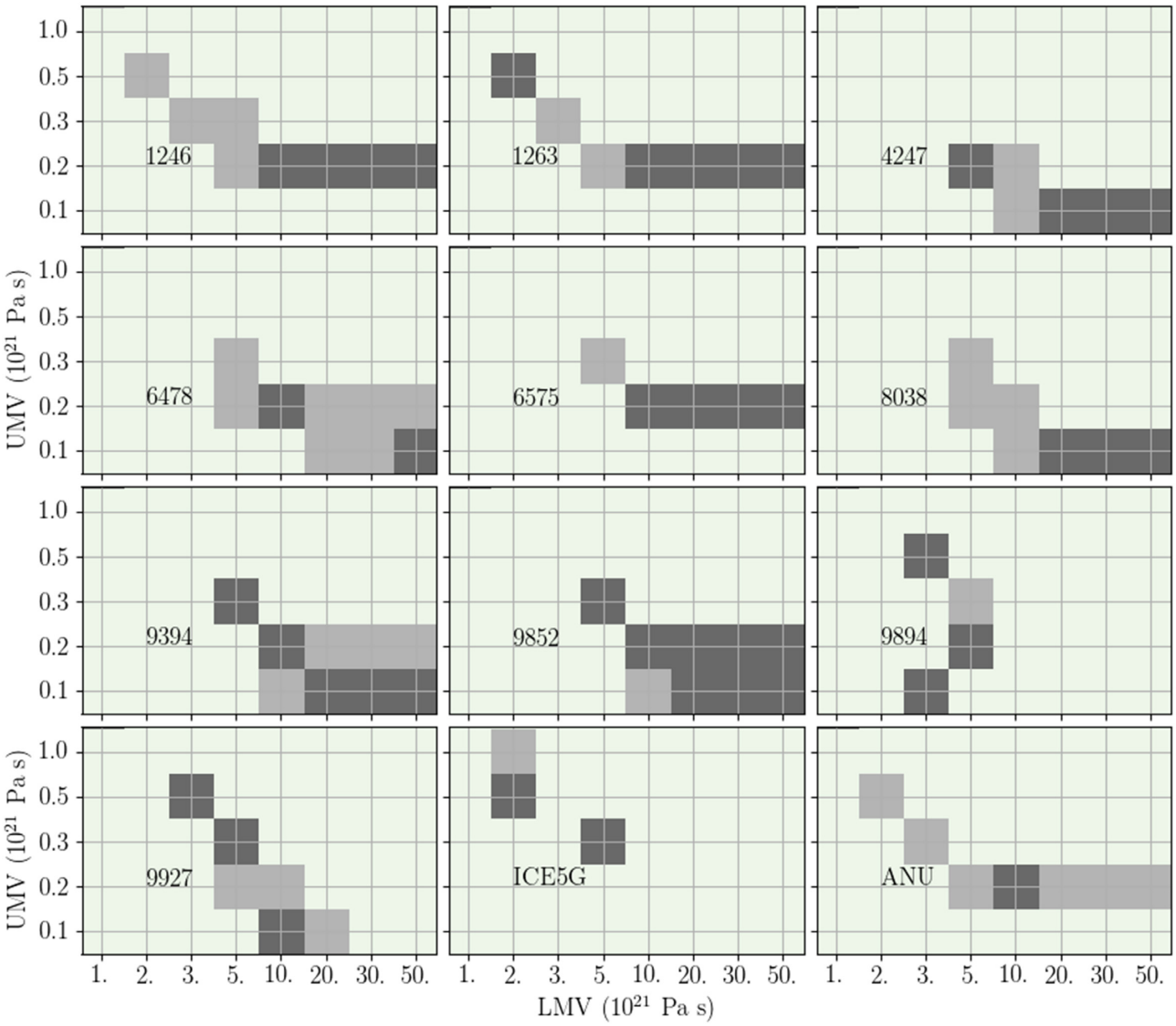

Figure 7. As in Fig. 6 but for the James Bay data.

times over raw RSL data is reduced. Of our three study sites, the least sensitivity of computed decay times to ice history is in Richmond Gulf. For this location, there are large regions of parameter space common to all ice models considered that satisfy the data. This can be considered either a positive or a negative result: On the one hand, this supports an interpretation of low functional ice sensitivity there, but on the other, the very large parameter solution space makes the Richmond Gulf decay time a weaker constraint on viscosity structure. Of course, a rigorous inversion for viscosity structure should include more than the decay time from a single region, and so Richmond Gulf would rarely be the only considered constraint.

If we consider regions of parameter space that show low ice sensitivity (e.g. consistency across ice models) that also satisfy the data in both Richmond Gulf and Ångerman River, then we find that models with a UMV of 0.3×10^{21} Pa s and an LMV of either 10×10^{21}or 20×10^{21} Pa s are consistent to both. This is broadly consistent with other inversions (e.g. Mitrovica & Forte 2004; Lau *et al.* 2016; Nakada *et al.* 2016), and indicates that while there are regions of parameter space that are more sensitive to the input ice history than others, this sensitivity does not seem to extend to the regions of parameter space most favoured by the data. However, the Richmond Gulf and Ångerman River decay times are reflective of their own local viscosity structure, and while it is consistent in our modelling framework to combine these constraints for a 1-D spherically symmetric Earth, it may not reflect the real Earth where viscosity structure exhibits lateral variation that can significantly affect decay time calculations (Lau *et al*. 2018; Kuchar *et al*. 2019). For example, Paulson *et al.* (2005) compare computed Hudson Bay decay times from a 3-D GIA model with those of 1-D models with viscous structure corresponding to global and regional averages identical to the 3-D model, and find nearly a 30 per cent misfit when comparing the 3-D model to its corresponding global average 1-D model, and a reduced but still significant 10 per cent misfit when comparing to the Hudson Bay regional average model.

3.2.1 Effects of Data Corrections

To conclude this section, we briefly discuss the impacts of the applied data corrections (Section 2.3). We have produced versions

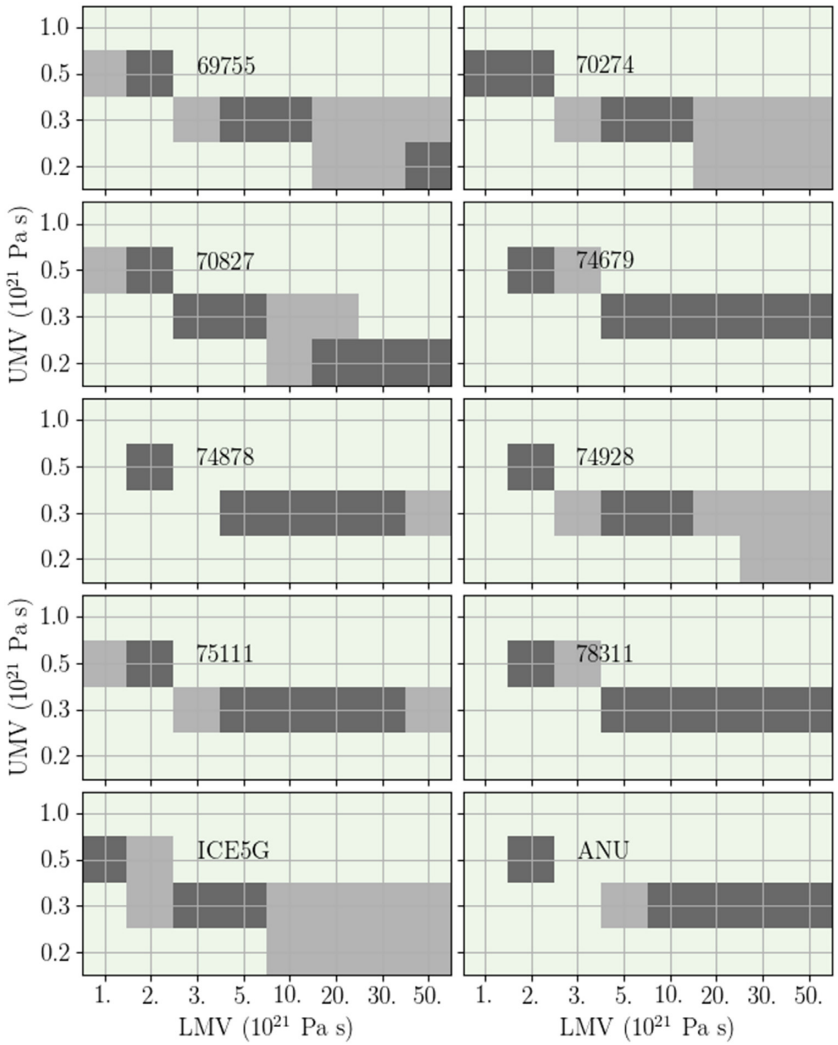

Figure 8. As in Fig. 6 but for the Ångerman River data.

of Figs 6 and 8 in the Supplemental material where: (i) we apply no corrections, the uncorrected data are fit alongside the full modelled sea level (model curve generated at the aggregate location shown in Fig. 1; Figs S6 and S7); (ii) only the correction defined in eq. (4) is applied to the data, which is then fit alongside the modelled ice component of the RSL (Figs S8 and S9) and (iii) only the spatial variability correction is applied to the data, which is then fit alongside the full RSL output (Figs S10 and S11). This analysis is performed only for Richmond Gulf and Ångerman River and not James Bay in part because the spatial correction was never applied to James Bay, and in part because it has already been discounted as a location that is well-suited to a decay time analysis.

When no corrections are applied to the Richmond Gulf data, the accepted regions on viscosity space are similar but there are also significant differences. The greatest changes, compared to the fully corrected case, are for the 8038 and 9852 ice histories. It is notable, however, that the same Earth models with a UMV of (0.3–0.5)x10^{21} Pa s are common to all ice models in both the uncorrected and fully-corrected cases. The uncorrected Ångerman River data lead to many of the models having the acceptable space of UMV values lowered from 0.3 to 0.2 $\times$ 10^{21} Pa s. The decreased sensitivity of Richmond Gulf relative to Ångerman River to the data corrections is likely due to the larger time uncertainties on the calibrated Richmond Gulf data leading to larger parameter uncertainties that dominate over the influence of biases in the uncorrected data. There are no viscosity models that are accepted universally by both the uncorrected Richmond Gulf and Ångerman River data.

When the correction defined in eq. (4) is applied, the acceptable model space for Richmond Gulf is, again, broadly similar to that for the fully corrected case. For Ångerman River the effect of this correction relative to the uncorrected case is to broaden the region of accepted parameters at lower UMV values. This suggests that the contribution from ocean loading can impact the viscosity inference at this location.

Finally, when only the spatial corrections are applied, there is a significant reduction in the size of the parameter solution space in Richmond Gulf relative to the uncorrected case. The acceptable models common to all ice histories still contain a UMV of 0.3 $\times$ 10^{21} Pa s and a LMV of at least 10 $\times$ 10^{21} Pa s, or a UMV of 0.5 $\times$ 10^{21} Pa s and a LMV of at least 3 $\times$ 10^{21} Pa s. For Ångerman River this correction has a less significant effect than in Richmond Gulf (though it does still change the solution space). This may be due to the amplitude of the spatial correction being larger at Richmond Gulf (see Fig. 1).

4 CONCLUSIONS

While RSL data are generally sensitive to both the Earth's viscosity structure and to the assumed ice history, postglacial decay times have been shown to reduce the sensitivity to the ice history. This makes decay times a useful parametrization for determining Earth viscosity. In this study we have investigated the extent of the sensitivity to the ice input by computing RSL histories and their corresponding exponential decay times for a suite of Earth viscosity profiles and ice histories. We have found that the exponential decay time characteristic to an RSL history is not generally independent of the ice history used to generate it. Moreover, the significant difference in decay times in James Bay and Richmond Gulf for identical Earth viscosity profiles suggests that the decay times computed at a given location may be more sensitive to position relative to the geometry of the ice sheet than has been suggested in the past. Our sensitivity analysis shows that Richmond Gulf decay times are relatively insensitive to ice history, confirming that data from this location are well-suited to a decay time analysis. In contrast, RSL data from James Bay are less well-suited because of the relatively large sensitivity of computed decay times to the input ice model at this location.

We have applied data corrections to account for the spatial distribution of RSL data over the study regions, as well as for the effects of the ocean load, rotation and changes in global mean sea level (associated with meltwater input and syphoning), so that only the local 'free decay' related to the removal of the ice load is considered in the decay time analysis. These corrections generally produce a greater effect on the estimated decay times in Ångerman River than in Richmond Gulf due, in part, to the lower temporal resolution of the RSL data in Richmond Gulf. However, the spatial correction has a stronger effect on the Richmond Gulf solution space owing to the relatively large area over which the data are distributed and the relatively large RSL gradient. While the load correction was applied in part to make the ice sensitivity easier to isolate, and is therefore likely not necessary in general, we do recommend the spatial correction for instances where RSL data is spread over a region with a significant RSL gradient.

We performed a forward modelling analysis to infer the viscosities in two sub-lithosphere layers (boundary at 670 km depth) that satisfy the decay time data. In general, the inferred range of Earth viscosity values that satisfy the RSL data constraints are ice history dependent to some extent. This analysis yielded regions of parameter space where solutions were common to all or most ice histories, indicating low ice sensitivity, as well as only subsets of ice histories, indicating relatively high sensitivity to the ice input. For example, in Richmond Gulf, UMV values of (0.3–0.5)x10^{21} Pa s and LMV values of (5–50)x10^{21} Pa s tend to satisfy the data constraints consistently for most ice histories. By contrast, only 5 of 12 ice histories demonstrate data-model agreement in the region defined by a UMV value of 10^{21} Pa s and LMV values of (30–50)x10^{21} Pa s. In James Bay there is only a small region of parameter space that satisfies the data, and only for 7 of the 12 ice histories considered. The Ångerman River solution spaces are generally narrower than those of Richmond Gulf, and all ice histories considered led to solutions with a UMV value of 0.5×10^{21} Pa s and LMV value of 2×10^{21} Pa s. There is an additional solution with a UMV value of 0.3×10^{21} Pa s and LMV values of (5–50)x10^{21} Pa s common to 9 of the 10 ice histories considered for this region. An important caveat is that our analysis has not checked the self-consistency of the ice model and Earth model sets under all the other geodetic and RSL constraints that went into their original development. Overall, this study indicates that joint calibration of ice sheet and Earth viscosity models for deglacial (or longer) contexts (e.g. Lambeck *et al*. 1998; Caron *et al*. 2017) is the optimal approach in near-field regions.

ACKNOWLEDGEMENTS

JK and GM acknowledge the National Science and Engineering Research Council and the University of Ottawa. We thank Erik Ivins and Jerry Mitrovica for providing detailed and constructive reviews of this work.

REFERENCES

Andrews, J.T., 1970. *A Geomorphological Study of Postglacial Uplift with Particular Reference to Arctic Canada,* Oxford University Press.

Boggs, P.T., Byrd, R.H., Rogers, J.E. & Schnabel, R.B, 1992. *User's Reference Guide for ODRPACK version 2.01: Software for Weighted Orthogonal Distance Regression,* Center for Computing and Applied Mathematics, U.S. Department of Commerce, Gaithersburg, MD.

Boggs, P.T., Donaldson, J.R., Byrd, R.H. & Schnabel, R.B., 1989. ALGORITHM 676 ODRPACK: software for weighted orthogonal distance regression, *ACM Trans. Math. Software,* **15,** 348–364.

Caron, L., Métivier, L., Greff-Lefftz, M., Fleitout, L. & Rouby, H., 2017. Inverting Glacial Isostatic Adjustment signal using Bayesian framework and two linearly relaxing rheologies, *Geophys. J. Int.,* **209,** 1126–1147.

Cathles, L.M., 1975. *The Viscosity of the Earth's Mantle,* Princeton University Press.

Dyke, A.S., 2004. An outline of North American deglaciation with emphasis on central and northern Canada, in *Quaternary Glaciations – Extent and Chronology, Part II,* ed. Ehlers, J. & Gibbard, P.L., Elsevier.

Dziewonski, A.M. & Anderson, D.L., 1981. Preliminary reference Earth model, *Phys. Earth planet. Inter.,* **25**(4), 297–356.

Han, H.K. & Gomez, N., 2018. The impact of water loading on postglacial decay times in Hudson Bay, *Earth planet. Sci. Lett.,* **489,** 1–10.

Hill, A.M., Milne, G.A., Kuchar, J. & Ranalli, G., 2018. Sensitivity of glacial isostatic adjustment to a partially molten layer at 410 km depth, *Geophys. J. Int.,* **216,** 3, 1538–1548

Hughes, A.L.C., Gyllencreutz, R., Lohne, Ø.S., Mangerud, J. & Svendsen, J.I., 2016. The last Eurasian ice sheets – a chronological database and time-slice reconstruction, DATED-1, *Boreas,* **45,** 1–45. ISSN 0300-9483.

Kendall, R.A., Mitrovica, J.X. & Milne, G.A., 2005. On post-glacial sea level - II. Numerical formulation and comparative results on spherically symmetric models, *Geophys. J. Int.,* **161**(3), 679–706.

Kuchar, J., Milne, G.A. & Latychev, K., 2019. The importance of lateral Earth structure for North American glacial isostatic adjustment, *Earth planet. Sci. Lett.,* **512,** 236–245.

Lambeck, K., 1993. Glacial rebound of the British Isles-11. A high resolution, high-precision model, *Geophys. J. Int.,* **115,** 960–990.

Lambeck, K., Purcell, A. & Zhao, S., 2017. The North American Late Wisconsin ice sheet and mantle viscosity from glacial rebound analyses, *Quat. Sci. Rev.,* **158,** 172–210.

Lambeck, K., Rouby, H, Purcell, A, Sun, Y. & Sambridge, M., 2014. Sea level and global ice volumes from the Last Glacial Maximum to the Holocene, *Proc. Nat. Acad. Sci.,* **111**(43), 15 296–15 303.

Lambeck, K., Smither, C. & Johnston, P., 1998. Sea-level change, glacial rebound and mantle viscosity for northern Europe, *Geophys. J. Int.,* **134,** 102–144.

Lau, H.C.P., Austermann, J., Mitrovica, J.X., Crawford, O., Al-Attar, D. & Latychev, K., 2018. Inferences of mantle viscosity based on ice age datasets: the bias in radial viscosity profiles due to the neglect of laterally heterogeneous viscosity structure, *J. geophys. Res.,* **123,** 7237–7252.

Lau, H.C.P., Mitrovica, J.X., Austermann, J., Al-Attar, D., Crawford, O. & Latychev, K., 2016. Inferences of mantle viscosity based on ice age data sets: radial structure, *J. geophys. Res.,* **121**(10), 6991–7012.

Love, R., Milne, G.A., Tarasov, L., Engelhart, S.E., Hijma, M.P., Latychev, K., Horton, B.P. & Törnqvist, T.E., 2016. The contribution of glacial isostatic adjustment to projections of sea-level change along the Atlantic and gulf coasts of North America, *Earth's Future,* **4**(10), 440–464.

McConnell, R.K., 1968. Viscosity of the mantle from relaxation spectra of isostatic adjustment, *J. geophys. Res.,* **73,** 7089–7105.
Milne, G.A. & Mitrovica, J.X., 1998. Postglacial sea-level change on a rotating Earth, *Geophys. J. Int.,* **133**(1), 1–19.
Mitrovica, J.X., 1996. Haskell [1935]revisited, *J. geophys. Res.,* **101**(B1), 555–569.
Mitrovica, J.X. & Forte, A.M., 1997. Radial profile of mantle viscosity: results from the joint inversion of convection and postglacial rebound observables, *J. geophys. Res.,* **102**(B2), 2751–2769.
Mitrovica, J.X. & Forte, A.M., 2004. A new inference of mantle viscosity based upon joint inversion of convection and glacial isostatic adjustment data, *Earth planet. Sci. Lett.,* **225,** 177–189.
Mitrovica, J.X., Forte, A.M. & Simons, M., 2000. A reappraisal of postglacial decay times from Richmond Gulf and James Bay, Canada, *Geophys. J. Int.,* **142**(3), 783–800.
Mitrovica, J.X. & Milne, G.A., 2003. On post-glacial sea level: I. General theory, *Geophys. J. Int.,* **154**(2), 253–267.
Mitrovica, J.X. & Peltier, W.R., 1993. A new formalism for inferring mantle viscosity based on estimates of post glacial decay times: application to RSL variations in N.E. Hudson Bay, *Geophys. Res. Lett.,* **20,** 2183–2186.
Mitrovica, J.X. & Peltier, W.R., 1995. Constraints on mantle viscosity based upon the inversion of post-glacial uplift data from the Hudson Bay region, *Geophys. J. Int.,* **122**(2), 353–377.
Mitrovica, J.X., Wahr, J., Matsuyama, I. & Paulson, A., 2005. The rotational stability of an ice-age Earth, *Geophys. J. Int.,* **161,** 491–506.
Nakada, M., Okuno, J. & Yokoyama, Y., 2016. Total meltwater volume since the Last Glacial Maximum and viscosity structure of Earth's mantle inferred from relative sea level changes at Barbados and Bonaparte Gulf and GIA-induced $\dot{J}_2$, *Geophys. J. Int.,* **204,** 1237–1253.
Nordman, M., Milne, G. & Tarasov, L., 2015. Reappraisal of the Ångerman River decay time estimate and its application to determine uncertainty in Earth viscosity structure, *Geophys. J. Int.,* **201**(2), 811–822.
Paulson, A., Zhong, S. & Wahr, J., 2005. Modelling post-glacial rebound with lateral viscosity variations, *Geophys. J. Int.,* **163,** 357–371.
Peltier, W.R., 1974. The impulse response of a Maxwell Earth, *Rev. Geophys.,* **12**(4), 649–669.
Peltier, W.R., 1996. Mantle viscosity and ice-age ice sheet topography, *Science,* **273,** 1359–1364.
Peltier, W.R., 1998. Postglacial variations in the level of the sea: Implications for climate dynamics and solid-earth geophysics, *Rev. Geophys.,* **36**(4), 603–689.
Peltier, W.R., 2004. Global glacial isostasy and the surface of the ice-age Earth: the ICE-5 G (VM2) model and GRACE, *Ann. Rev. Earth planet. Sci.,* **32,** 111–149.
Peltier, W.R. & Andrews, J.T., 1976. Glacial isostatic adjustment - I. The forward problem, *Geophys J.R. astr. Soc.,* **46,** 605–646.
Peltier, W.R. & Drummond, R., 2008. Rheological stratification of the lithosphere: a direct inference based on the geodetically observed pattern of the glacial isostatic adjustment of the North American continent, *Geophys. Res. Lett.,* **35,** doi:10.1029/2008GL034586.
Peltier, W.R., Shennan, I., Drummond, R. & Horton, B.P., 2002. On the postglacial isostatic adjustment of the British Isles and the shallow viscoelastic structure of the Earth, *Geophys. J. Int.,* **148,** 443–475.
Pendea, I.F., Costopoulos, A., Nielsen, C. & Chmura, G.L., 2010. A new shoreline displacement model for the last 7 ka from eastern James Bay, Canada, *Quat. Res.,* **73**(3), 474–484.
R Core Team, 2018. *R: A Language and Environment for Statistical Computing,* R Foundation for Statistical Computing, Vienna, Austria.
Reimer, P.J. *et al.*, 2013. IntCal13 and Marine13 radiocarbon age calibration curves 0–50 000 years cal BP, *Radiocarbon,* **55**(4), 1869–1887.
Roy, K. & Peltier, W.R., 2015. Glacial isostatic adjustment, relative sea level history, and mantle viscosity: reconciling relative sea level model predictions for the U.S. East coast with geological constraints, *Geophys. J. Int.,* **201,** 1156–1181.
Sella, G.F., Stein, S., Dixon, T.H., Craymer, M., James, T.S., Mazzotti, S. & Dokka, R.K., 2007. Observation of glacial isostatic adjustment in "stable" North America with GPS, *Geophys. Res. Lett.,* **34,** doi:10.1029/2006GL027081.
Steffen, H. & Kaufmann, G., 2005. Glacial isostatic adjustment of Scandinavia and northwestern Europe and the radial viscosity structure of the Earth's mantle, *Geophys. J. Int.,* **163,** 801–812.
Stuiver, M. & Reimer, P.J., 1993. Extended C14 data base and revised calib 3.0 C14 age calibration Program, *Radiocarbon,* **35,** 215–230.
Tarasov, L., 2013. GLAC-1b: A new data-constrained global deglacial ice sheet reconstruction from glaciological modelling and the challenge of missing ice, *Eur. Geophys. Un. Gen. Assembly 2013, Abstracts,* **15,** EGU2013–12342.
Tarasov, L., Dyke, A.S., Neal, R.M. & Peltier, W., 2012. A data-calibrated distribution of deglacial chronologies for the North American ice complex from glaciological modeling, *Earth planet. Sci. Lett.,* **315–316,** 30–40.
Tromp, J. & Mitrovica, J.X., 1999. Surface loading of a viscoelastic earth—I. General theory, *Geophys. J. Int.,* **137,** 847–855.
Tushingham, A.M. & Peltier, W.R., 1991. ICE-3G: a new global model of late Pleistocene glaciation based upon geophysical predictions of postglacial relative sea level change, *J. Geophys. Res.,* **96,** 4497–4523.
Walcott, R.I., 1980. Rheological models and observational data of glacio-isostatic rebound, *Earth Rheology, Isostasy, and Eustasy,* pp. 3–10, ed. Morner, N.-A., John Wiley.

SUPPORTING INFORMATION

Supplementary data are available at *GJI* online.

Table S1. The RSL data used for Richmond Gulf, with C14 ages from Mitrovica *et al.* (2000) calibrated using the marine calibration curve of Reimer *et al.* (2013) and the Calib software (Stuiver & Reimer 1993). All ages given in thousands of years BP.
Figure S1. The reconstructions of the North American Ice Sheet (NAIS) used in this study shown at 20 ka BP (See main text for details). The first ten shown are reconstructions from Tarasov *et al.* (2012).
Figure S2. As in Fig. S1, but for the Fennoscandian Ice Sheet. The first eight shown are reconstructions from Tarasov (2013).
Figure S3. The standard deviation of decay times among ice histories for each study site. The structure is similar to the spread in decay time values (main text, Fig. 5), with Richmond Gulf showing the least amount of ice sensitivity.
Figure S4. Expanded version of Fig. 6 from main text, showing RSL in North America at 7 ka, for an Earth model with a 0.5 x 10^{21} Pa s UMV and a 10^{22} Pa s LMV.
Figure S5. Samples of corrected RSL data for Richmond Gulf (top panel) and James Bay (middle panel) and Ångerman River (bottom panel) with their associated best fit curves, for an earth model with a 3 x 10^{20} Pa s UMV and 10^{22} Pa s LMV and the 4247 ice history of Tarasov *et al.* (2012) for the Hudson Bay sites and the 70 274 ice history of Tarasov (2013) for Ångerman River. The estimated decay times are 5.0 $\pm$ 1.5 ka for Richmond Gulf, 3.67 $\pm$ 0.17 ka for James Bay and 4.52 $\pm$ 0.71 ka for Ångerman River.
Figure S6. Model-data agreement map for Richmond Gulf but with no corrections applied to the data and the full RSL model output used [i.e. RSL_{full} in eq. (4)]. The ice histories are labelled in each panel, and the numbered models are the reconstructions of Tarasov *et al.* (2012). Light grey indicates data-model agreement to within 2σ, while dark grey indicates agreement to within 1σ.
Figure S7. As in Fig. S6, but for Angerman River. The ice histories are labelled in each panel, and the numbered models are the reconstructions of Tarasov (2013).
Figure S8. As in Fig. S6, but with the correction defined by eq. (4) applied to the data, and only the modelled ice component of RSL considered [i.e. RSL_{ice} in eq. (4)].
Figure S9. As In Fig. S8, but for Angerman River.

Figure S10. As in Fig. S6, but with only the correction for spatial variability applied to the data, and compared to the full modelled RSL (i.e. RSL_{full} in eq. 4).
Figure S11. As in Fig. S10, but for Angerman River.